Faraday Discussions

Accepted Manuscript

Faraday Discussions

Royal Society of Chemistry

ROYAL SOCIETY OF CHEMISTRY

www.rsc.org/faraday_d

Ammonia decomposition catalysis using lithium-calcium imide

Joshua W. Makepeace[1,2], Hazel M. A. Hunter[2], Thomas J. Wood[2], Ronald I. Smith[2], Claire A. Murray[3]
and William I.F. David[1,2]*

[1]Inorganic Chemistry Laboratory, University of Oxford, South Parks Road, Oxford, OX1 3QR, UK
[2]ISIS Facility, Rutherford Appleton Laboratory, Harwell Campus, Didcot, OX11 0QX, UK
[3]Diamond Light Source Ltd, Rutherford Appleton Laboratory, Harwell Campus, Didcot, OX11 0DE, UK
* email bill.david@stfc.ac.uk

Abstract

Lithium-calcium imide is explored as a catalyst for the decomposition of ammonia. It shows the highest ammonia decomposition activity yet reported for a pure light metal amide or imide, comparable to lithium imide-amide at high temperature, with superior conversion observed at lower temperatures. Importantly, the post-reaction mass recovery of lithium-calcium imide is almost complete, indicating that it may be easier to contain than the other amide-imide catalysts reported to date. The basis of this improved recovery is that the catalyst is, at least partially, solid across the temperature range studied under ammonia flow. However, lithium-calcium imide itself is only stable at low and high temperatures under ammonia, with *in-situ* powder diffraction showing the decomposition of the catalyst to lithium amide-imide and calcium imide at intermediate temperatures of 200–460 °C.

Introduction

The catalytic decomposition of ammonia to release its stored hydrogen is an important step in enabling the use of ammonia as a potential replacement for fossil fuels in technologies ranging from transportation to seasonal energy storage. The partial decomposition of ammonia when used in an internal combustion engine enables more favourable combustion conditions to be used[1], while low-temperature fuel cells require the complete decomposition of ammonia to hydrogen and nitrogen:

$$2NH_3 \rightarrow N_2 + 3H_2 \qquad (1).$$
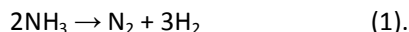
Using current catalyst technology, the kinetics of ammonia decomposition are slow and require very high operating temperatures that, in turn, compromise the efficiency of the ammonia-based energy cycle[2]. The development of affordable catalysts with higher activity can therefore represent a significant step in facilitating the widespread use of ammonia as a sustainable fuel.

Currently, the most active catalysts for ammonia decomposition involve transition metals[3] and use a range of support architectures (such as porous carbon, metal oxides and carbon nanotubes[4]) along with alkali- and alkaline earth-metal salts[5,6] to enhance activity. Among the metals studied, ruthenium, nickel and iron have been the most widely investigated. Ruthenium is generally considered to be the most active metal per mole while iron-based catalysts are favourable per unit mass since their cost advantage over ruthenium allows the use of higher metal loadings.

Light metal amides and imides have recently emerged as a new class of catalyst for the decomposition of ammonia. While the precise mechanism of their catalytic action is not yet fully elucidated, sodium amide ($NaNH_2$)[7], lithium imide (Li_2NH)[8] and composites of lithium imide with transition metals and their nitrides[9,10] show high ammonia decomposition activity. There are

indications from isotope exchange measurements that these materials have a more complex interaction with ammonia than that of simple surface catalysis and that there are bulk interactions between the catalysts and the ammonia to which they are exposed[8,11]. The active forms of the catalysts are dependent on the precise ammonia decomposition conditions (ammonia flow rate, temperature). For the sodium amide system a mixture of sodium and sodium amide is observed[7] while a non-stoichiometric lithium imide ($Li_{1+x}NH_{2-x}$, $0 \leq x \leq 1$) is seen in the lithium-based system[8]. Composites of lithium imide with metal nitrides, which show an enhanced activity, have been proposed to form a ternary nitride during ammonia decomposition[9].

There are many avenues for the further development of these catalysts in order to provide a low-cost and effective method of releasing hydrogen from ammonia. One challenge encountered with the sodium/sodium amide system is that both components of the system are liquid at the temperature of operation; indeed, sodium itself has a vapour pressure in the order of 25 mbar at 600 °C[12], leading to issues associated with catalyst containment within the heated reaction zone. While a reflux-type arrangement may help contain a liquid catalyst, it is anticipated this would reduce the efficiency of the reaction and may introduce overly complex engineering requirements.

Stoichiometric lithium imide is solid across the temperature range in which the ammonia decomposition reaction occurs. However, the reaction with ammonia to form a non-stoichiometric phase

$$Li_2NH + NH_3 \rightarrow 2LiNH_2 \qquad (2),$$
$$xLiNH_2 + (1-x)Li_2NH \rightarrow Li_{2-x}NH_{1+x} \qquad (3),$$
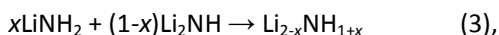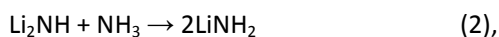
introduces lithium amide-like character to the catalyst structure. Lithium amide melts at around 370 °C. In an *in-situ* neutron powder diffraction experiment, it was observed that a stoichiometry value close to $Li_{1.5}ND_{1.5}$ was the approximate limit of maintaining a solid phase at 500 °C under very low ammonia flows (of around 5 standard cubic centimetres per minute, sccm)[8]. This evidence indicates that the ammonia decomposition reaction conditions must be maintained within specific limits if the catalyst is to be kept in the solid state during the reaction.

A logical progression from this work is to examine related materials which may be easier to maintain as a solid. In particular, imide materials have much higher melting points than their corresponding amides, and so an imide which forms at low temperature would seem to be an ideal candidate for a practical ammonia decomposition catalyst. Taking the example of the lithium amide–lithium hydride hydrogen storage system[13], reductions in the hydrogen desorption temperature (*i.e.* a lower temperature of imide formation) were achieved by using ternary systems combining lithium amide with magnesium hydride[14,15] or calcium hydride[16,17]. Of particular interest to this study is that a 2:1 mixture of lithium amide with the relevant hydride results in the formation of a ternary imide:

$$2LiNH_2 + MgH_2 \rightarrow Li_2Mg(NH)_2 + 2H_2 \qquad (4).$$
$$2LiNH_2 + CaH_2 \rightarrow Li_2Ca(NH)_2 + 2H_2 \qquad (5).$$
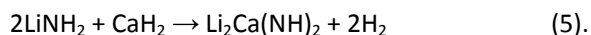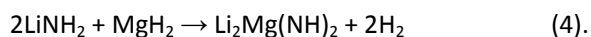
The lower temperatures of these reactions compared with the lithium-only analogue raise the prospect that these imides may be more stable in the presence of ammonia than lithium imide alone. The elevated pressures required to hydrogenate these ternary imides relative to lithium imide may indicate that this hypothesis has merit; however, there are no studies to date that examine

their interaction with ammonia. The aim of this work is to examine the ammonia decomposition properties of these two ternary imides with a focus on whether they offer enhanced practicality compared to lithium imide.

Experimental

Sample preparation

All sample preparation and handling was undertaken inside an argon-filled glove box (Unilab, mBraun, O_2 and H_2O <0.1 ppm). Samples of lithium-calcium imide were prepared by the reaction of lithium amide ($LiNH_2$, 98 %, Sigma Aldrich) and calcium hydride (CaH_2, 98 %, Sigma Aldrich). The powdered reactants were mixed in a 2:1 molar ratio by hand using an agate mortar and pestle for 5 minutes per gram of reactant mixture. 2 g of the resultant mixture was loaded into a 125 mL tungsten carbide (WC) milling jar filled with nine 10 mm tungsten carbide milling balls. The sample was milled under argon in the WC jar for four hours at 400 rpm in a Retsch PM100 planetary mill, in 15 minute segments with two minute rest periods between each segment. The direction of rotation was reversed after each segment. The ball-milled mixture was then heated in 0.25 g portions to affect the reaction to form lithium-calcium imide (equation 5).

The portion was placed in a cylindrical alumina crucible housed inside a quartz tube. The sample was put under flowing argon gas (99.998 %, BOC), placed inside a horizontal tube furnace (Carbolite MTF 12/38/400) and heated to 380 °C at a ramp rate of 2 °C/min and held at that temperature for 12 hours. Powder X-ray diffraction (XRD) of the samples, performed on a PANalytical X'Pert diffractometer using copper $K\alpha_1$ radiation, confirmed that the synthesised lithium-calcium imide was at least 90 % pure as assessed by Rietveld analysis of the powder pattern with the TOPAS Academic v5.0 package (see ESI).

Lithium-magnesium imide was synthesised in an analogous fashion to lithium-calcium imide, using magnesium hydride (MgH_2, 98 %, Aldrich) in place of calcium hydride.

A sample of deuterated lithium-calcium imide ($Li_2Ca(ND)_2$) was prepared for the neutron powder diffraction measurement. The synthesis method was as described above, using the deuterated isotopomers of the starting materials. Deuterated lithium amide ($LiND_2$) was prepared by the reaction of lithium nitride (Li_3N, 98 %, Sigma Aldrich) with deuterated ammonia (ND_3, 99 %, 99 atom% D, Aldrich):

$$Li_3N + 2ND_3 \rightarrow 3LiND_2 \qquad (6).$$

A hand-ground 1 g sample of lithium nitride was placed in a cylindrical stainless steel reactor, sealed and attached to the deuterated ammonia supply. The system was evacuated and then filled with 3 bar of ammonia, heated at 5 °C/min to 300 °C and held at that temperature for 3 hours. The resultant powder was confirmed to be deuterated lithium amide by XRD and Raman spectroscopy (Bruker Senterra).

Calcium deuteride (CaD_2) was prepared by the reaction of *ca.* 1 mm pieces of calcium metal (99.5 %, Alfa Aesar) with deuterium gas (D_2, 99.8 atom% D, SIP Analytical). The calcium pieces were used as-received and were placed into a cylindrical stainless steel reactor, sealed and attached to the deuterium supply. The system was evacuated and then filled with 10 bar of deuterium. The sample

was subsequently heated at 5 °C/min to 315 °C and held at that temperature overnight. The composition of the resultant off-white powder was confirmed as calcium deuteride by XRD.

The purity of the deuterated lithium-calcium imide synthesised from the reaction of these starting materials was confirmed to be in excess of 90 % by XRD (see ESI).

Ammonia decomposition testing

The ammonia decomposition testing used an identical setup to that described previously[7,8]. Catalyst powders were loaded into a 46.9 cm^3 cylindrical nickel-plated 316 stainless steel reactor with gas flow input along a pipe through the centre of the cylinder, entering 1 cm from the bottom of the reactor (see ESI). Out flow was through the lid of the reactor. Gas flow of argon or ammonia (NH_3, 99.999 %, SIP Analytical) was controlled using a mass flow controller (HFC-302, Teledyne Hastings Instruments) housed in a custom-designed gas panel. The reactor was heated using a vertical tube furnace (Severn Thermal Solutions). The composition of the gas leaving the reactor was analysed using a Quantitative Gas Analyser mass spectrometry system (HPR20 QIC R&D, Hiden Analytical), run in multiple ion detection mode with a Faraday detector. Mass-to-charge ratios (*m/z*) corresponding to hydrogen (*m/z* = 2), ammonia (*m/z* = 17), nitrogen (*m/z* = 28) and argon (*m/z* = 40) were monitored. In a typical ammonia decomposition experiment, ammonia was flowed at 60 sccm through the system and the reactor was heated in steps between 250 °C and 600 °C, with 3 hour dwell periods at each temperature set point.

Ammonia decomposition percentages were calculated using an in-house computer program which removes the background signal for each species and calculates the ammonia decomposition percentage based on the average value over the dwell period at each temperature set point.

Synchrotron X-ray powder diffraction

Two synchrotron X-ray powder diffraction experiments were performed on the I11 beam line at the Diamond Light Source, United Kingdom. Diffraction data were collected in 2 minute intervals using the multi-analyser crystal (MAC) detectors and an X-ray wavelength of 0.826209 Å was used.

For each experiment, a sample of lithium-calcium imide was placed in the centre of a 0.9 mm i.d. single crystal sapphire capillary, which was open at both ends. The powder sample was held in position by a plug of quartz wool on either side. The capillary was loaded into a flow-through gas cell and mounted on the beam line (see ESI). After leak testing with helium gas, the sample was aligned and a hot air blower was positioned to heat the sample. The sample was rocked between -5 and +15 ° to minimise preferred orientation effects during data collection.

In the first experiment, the sample of lithium-calcium imide was heated from room temperature to 550 °C at 5 °C/min under a constant flow of 1 sccm of helium gas. The sample was held at 550 °C for half an hour and then cooled to room temperature at 10 °C/min. In the second experiment, the sample was heated under a 1 sccm flow of ammonia, initially to 350 °C at 5 °C/min, with a one hour dwell at that temperature. Subsequently, the sample was heated in 50 °C steps at 5 °C/min with one hour dwells at each temperature, up to a maximum temperature of 600 °C. Finally, the sample was cooled at 10 °C/min.

Differential scanning calorimetry–thermogravimetric analysis

A Netsch STA 441 F1 Jupiter was used for simultaneous differential scanning calorimetry and thermogravimetric analysis of lithium-calcium imide samples. 8.7 mg samples of the lithium-calcium imide were sealed inside 20 μL aluminium pans. The lid of each pan was pierced as it was loaded into the instrument. A purge flow of nitrogen gas was used during sample loading to protect the sample from moisture in the atmosphere. Once loaded, the sample was heated from 25 °C to 575 °C at 5 °C/min under a 20 sccm flow of either nitrogen or ammonia gas flow. The sample mass and relative heat flow to the sample pan were recorded throughout the experiment.

Neutron powder diffraction

In-situ time-of-flight neutron powder diffraction data for lithium-calcium imide were collected on the POLARIS instrument at the ISIS Neutron and Muon Source in the United Kingdom. The experimental setup for the *in-situ* experiment was very similar to that described previously when studying lithium imide[8]. The sample of deuterated lithium-calcium imide (1.9 g) was loaded into a stainless steel flow-through cell (see ESI) which was placed into a standard furnace housed in the POLARIS sample tank. Neutron diffraction data were collected in 100 s intervals throughout, and the furnace set to the desired temperature (or temperature ramp rate). The sample cell was attached to the same gas delivery panel, as used for ammonia decomposition testing, equipped with argon, ammonia and deuterated ammonia input gases. Outgas composition and ammonia decomposition percentages were calculated as described for the ammonia decomposition experiments. Given that deuterated species were used in the neutron diffraction experiment, the following mass-to-charge (m/z) fragments were analysed in addition to the standard fragments: ND_3 (m/z = 20), ND_2H (m/z = 19), NDH_2 (m/z = 18), D_2 (m/z = 4) and HD (m/z = 3), with the partially-deuterated species (and NH_3/H_2) included for monitoring during the H-D exchange experiment. Additionally a reference neutron powder diffraction dataset was collected of the as-prepared sample in a 6 mm vanadium can over 2 hours at room temperature.

Results and Discussion

The variable-temperature ammonia conversion percentages of lithium-calcium imide and lithium-magnesium imide are shown in Figure 1, with datasets for lithium amide and that of the blank reactor shown for comparison.

Below 430 °C, both lithium-calcium imide and lithium-magnesium imide show superior conversion activity to lithium imide-amide and very similar activity to each other. Above this temperature, the activity of lithium-magnesium imide is significantly lower than both lithium imide-amide and lithium-calcium imide. In contrast, above 430 °C the ammonia decomposition activity of lithium-calcium imide is very similar to that of lithium imide-amide. Overall, the variable-temperature ammonia conversion percentage profile of lithium-calcium imide in this system is the highest observed to date out of the pure metal amide or metal imide systems studied.
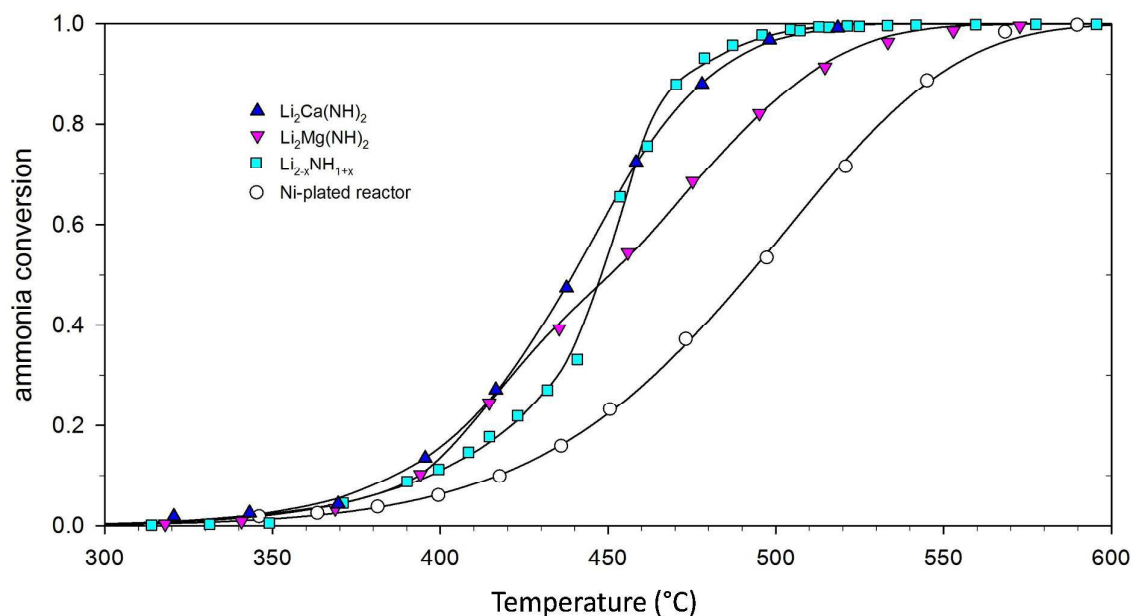
Figure 1 - Ammonia conversion fraction as a function of temperature for a number of metal amide/imide catalysts, along with the nickel-plated blank reactor. Measurement conditions were 0.5 g of catalyst and an ammonia flow rate of 60 sccm. The lines indicate the fits to the data.

In the published reports of the ammonia decomposition activity of light metal amides and imides there has been some disagreement as to how active the materials are on their own. It has been reported that composites of lithium amide-imide with transition metal nitrides display synergistic ammonia decomposition activity[9,10]. These results, measured for intimate mixtures, were used to infer that measurements in stainless steel reactors, such as those in this study and our previously-reported work, were not measuring the isolated activity of the amide/imide. Measurements of the activity of lithium amide-imide in quartz reactors show very low ammonia decomposition activity. Of course, it is difficult to isolate the effect of the reactor from the catalyst. In most cases, quartz is an inert material which is a good choice for reactors for ammonia decomposition. However, in our laboratory tests we have established that lithium amide and sodium amide react strongly with quartz at elevated temperature (see ESI), forming oxide and unknown phases that are most likely metal silicates. This may go some way to explain the very low ammonia decomposition activity observed for lithium and sodium amides when tested in quartz reactors. It is for this reason that this work continues the use of metal reactors for measuring ammonia decomposition activity. The interaction between metals/metal nitrides and these catalysts is of great interest, but experimental results to date suggest that the amide materials are actively decomposing ammonia, rather than playing a simple promotion role (as is the case with other Group I and II metal salts[18])[11]. Indeed, a recent study on the interaction of ruthenium with lithium amide-imide suggested that the enhanced ammonia decomposition activity from the composite material may in fact be due to the metal influencing the decomposition pathway of lithium amide[19].

To provide a quantitative measure of the data presented in Figure 1, the ammonia decomposition data were fitted by a least-squares procedure to one- or two-process sigmoidal functions of the form:

$$C_i = 1 - \exp(-\exp(A/R - E_A/RT)) \quad (7),$$

where C_i is the conversion (1 - ammonia fraction), A is a constant, R is the gas constant, E_A is an activation energy and T is the temperature (in Kelvin). Two-process functions were fitted to a sum of two equations shown in Equation 7, with different refined A and E_A values for each, with the total function given by:

$$C_{total} = 1 - [fC_1 + (1 - f)C_2] \qquad (8),$$

where f is the fractional contribution of the first sigmoidal function and 1-f is the fractional contribution of the second function. The outputs of the fitting process are summarised in Table 1.

Table 1 - Parameters from least-squares optimisation of sigmoidal functions fitted to variable-temperature ammonia conversion data . Uncertainties are given in brackets.

Species	A_1	E_{A1}	A_2	E_{A2}	f
$Li_2Ca(NH)_2$	0.16(2)	120(10)	0.28(3)	200(30)	0.70(4)
$Li_2Mg(NH)_2$	0.15(1)	112(11)	0.61(4)	421(30)	0.85(4)
$Li_{1+x}NH_{2-x}$	0.165(3)	120(4)	0.67(2)	490(17)	0.573(5)
Blank	0.141(9)	110(7)			

As outlined previously, one of the challenges with the use of light metal amides and imides for ammonia decomposition is containing the catalyst melt within the reactor hot zone. It is known[8] that lithium imide-amide can be kept solid under controlled conditions. When it is heated under argon to the temperature of high ammonia conversion, lithium imide will remain solid, and so mass recovery from the reactor is generally in excess of 80 %. In contrast, if it is heated under ammonia, the mass recovery is generally less than 30 % due to the formation and subsequent melting of lithium amide[8]. The mass recovery of the lithium-calcium imide sample after the ammonia decomposition reaction shown in Figure 1 was almost complete (98 %), whereas the lithium-magnesium imide recovery was less than 5 %. The combination of high activity and high mass recovery—which implies ease of containment—makes lithium-calcium imide worthy of further investigation as an attractive ammonia decomposition catalyst. Since lithium-magnesium imide showed neither of these attributes, it was not investigated further in this study.

The high mass recovery obtained for lithium-calcium imide is consistent with the catalyst remaining solid throughout the range of conditions used in the ammonia decomposition experiment. However, a post-reaction X-ray powder diffraction pattern, shown in Figure 2, indicates a more complex behaviour. Specifically, a mixture of lithium amide and calcium imide was identified, with no lithium-calcium imide observed in the diffraction pattern.
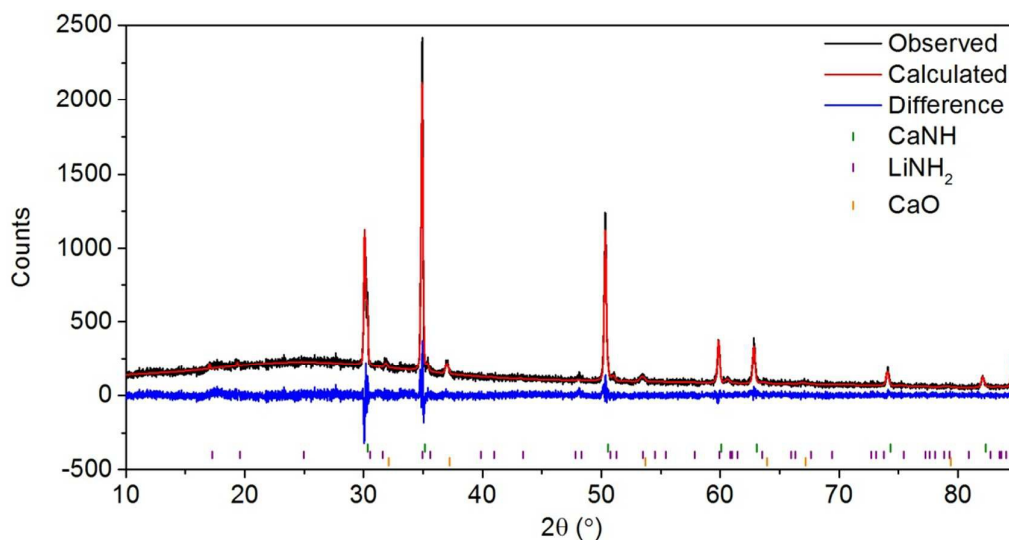
Figure 2 - X-ray powder diffraction pattern of the lithium-calcium imide catalyst after the ammonia decomposition reaction.

In order to provide more detailed information on this transformation and to gain an understanding of the active form of the catalyst and its practical limitations, *in-situ* diffraction experiments were undertaken. In the first experiment using synchrotron X-ray powder diffraction, lithium-calcium imide was heated under a 1 sccm flow of helium gas to examine whether simple heating could cause the material to separate into lithium imide and calcium imide. The published crystal structure of lithium-calcium imide, Figure 3, is a layered structure which can be described as alternating layers of lithium imide and calcium imide. As such, it is possible that the separation of those layers into the constituent imide phases may not require a large input of energy. After separation, lithium imide would readily react with ammonia to form lithium amide, consistent with the powder diffraction pattern obtained for the post-reaction sample.
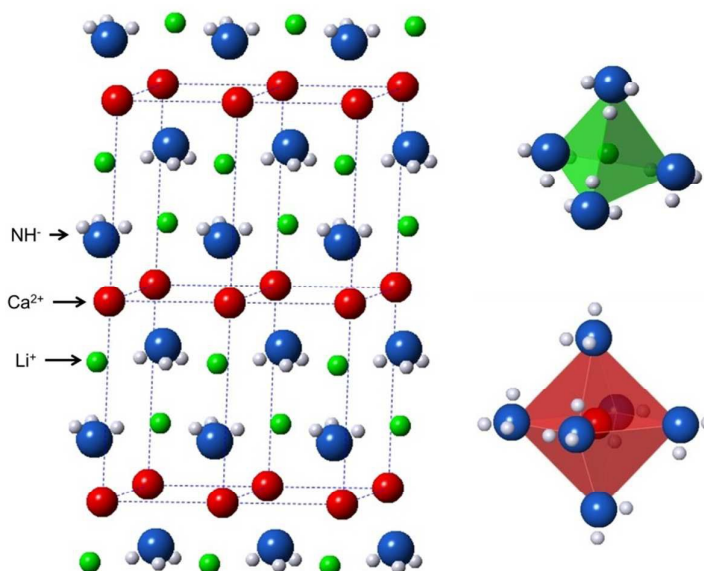
Figure 3 - Crystal structure of lithium-calcium imide, with lithium atoms shown in green, calcium in red, nitrogen in blue and hydrogen in grey. The local geometries of the Li(NH)$_4$ tetrahedron and Ca(NH)$_6$ octahedron are shown to the right.

A contour plot of the diffraction data for the heating of lithium-calcium imide between room temperature and 550 °C under helium is shown in Figure 4. What is immediately apparent from these data is that lithium-calcium imide is present over the entire temperature range and does not transform into lithium imide and calcium imide. Therefore it is reasonable to conclude that the decomposition of the catalyst is due to its interaction with ammonia.
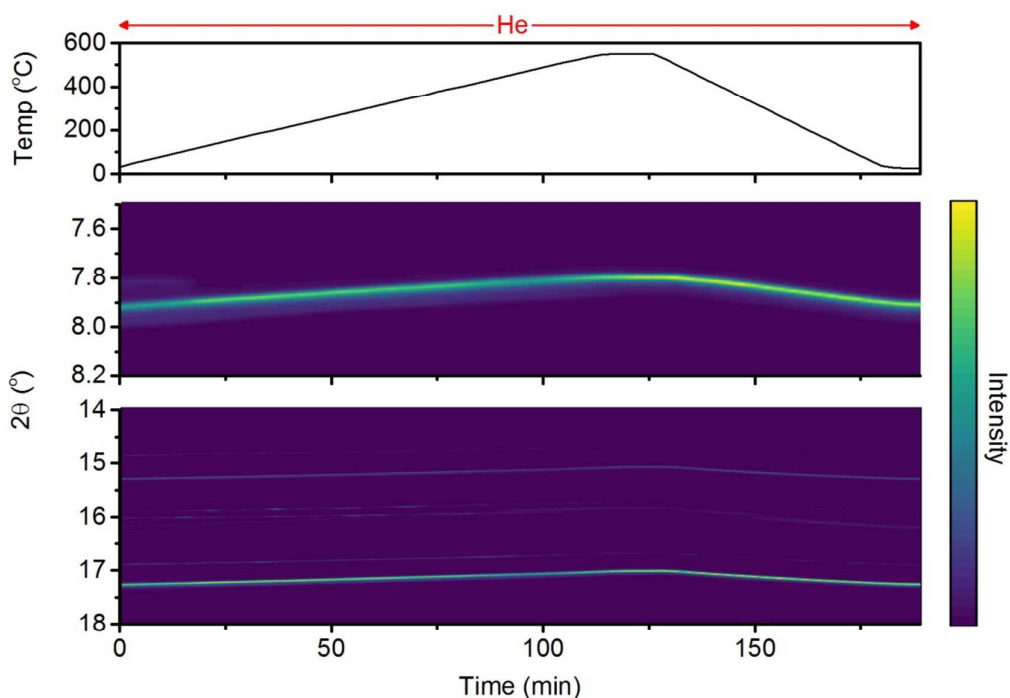

Figure 4 - Contour plot of sections of the *in-situ* synchrotron X-ray powder diffraction data for lithium-calcium imide. The sample was heated at 5 °C/min under 1 sccm flowing helium gas.

It is worth noting a few points regarding the structural characterisation of lithium-calcium imide from these data. A small shoulder is present on a number of the Bragg peaks associated with the lithium-calcium imide phase. An example of this feature as observed for the (001) peak is shown in Figure 5. As can be seen, the feature at 7.84° was present in the data until approximately 120 °C and not observed during the remainder of the experiment, even after the sample was cooled back to below 120 °C. It is thus unlikely that these extra peaks are related to an order-disorder transition similar to the transition observed in lithium imide at a slightly lower temperature[20]. Given the layered structure of the material, the most likely explanation for these features is that the initial sample possessed stacking faults which were annealed out of the structure.

Combined DSC-TGA of the sample (see ESI) also indicated the presence of an endothermic event at 86 °C which is consistent with an order-disorder transition of the lithium imide impurity in the sample. Annealing of stacking faults in the sample would be expected to be exothermic, but no thermal events were observed around the temperature of the loss of the low-angle shoulder. The DSC-TGA data also show no significant mass loss, consistent with the stability of the catalyst over the temperature range.

Further peak asymmetry is observed in the data comprising a small shoulder at higher 2-theta values, see Figure 5. This feature was particularly prevalent in the [00*l*] reflections and persisted throughout the experiment. This may be indicative of a degree of compositional variation or disorder in the lithium-calcium imide structure—for example a degree of non-stoichiometry could be envisaged similar to that observed in lithium imide[21–23]. This peak asymmetry was modelled in the Rietveld analysis of the diffraction data as a second component to the lithium-calcium imide phase, one with a very similar *a* lattice parameter to the main phase and a smaller (approx. 0.5 %) *c* lattice parameter.
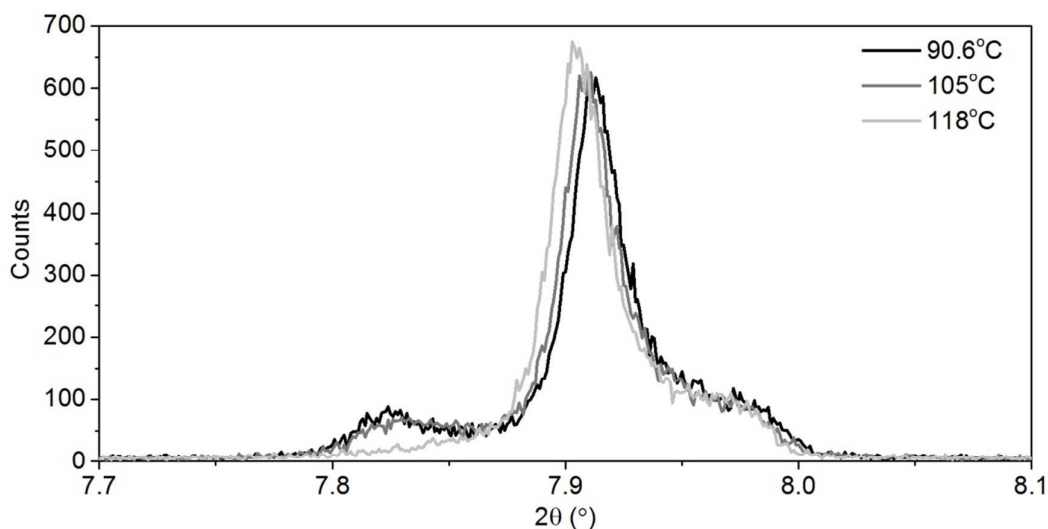

Figure 5 - The synchrotron X-ray powder diffraction (001) peak of lithium-calcium imide, showing the disappearance of the low-angle shoulder with heating under 1 sccm flowing helium, and the presence of high-angle asymmetry.

A plot of the variation in these refined parameters with temperature is shown in Figure 6. The *a* lattice parameters of the two components of lithium-calcium imide are close in magnitude and show similar thermal expansion behaviour. The *c* lattice parameter of the minor component is slightly

smaller than that of the major component. Figure 6 illustrates the differing thermal expansion behaviour of the two components. Upon heating, the major component displays almost linear thermal expansion behaviour, with a subtle change in the slope of the expansion at 120 °C, consistent with the disappearance of the low-angle asymmetry attributed to stacking faults in the structure. The minor component exhibits relatively steep thermal expansion behaviour below 180 °C during heating. Above this temperature, the rate of thermal expansion decreases to a similar rate to the major component. On cooling, both components display linear thermal contraction. The irreversible steep thermal expansion of the *c* axis of the minor component towards the value of the major component is consistent with the hypothesis that this asymmetry reflects compositional disorder in the structure which partially orders as the sample was heated at the beginning of the experiment. This partial ordering results in a narrowing of the Bragg peak, which produces the shift in the *c* parameter of the minor component.
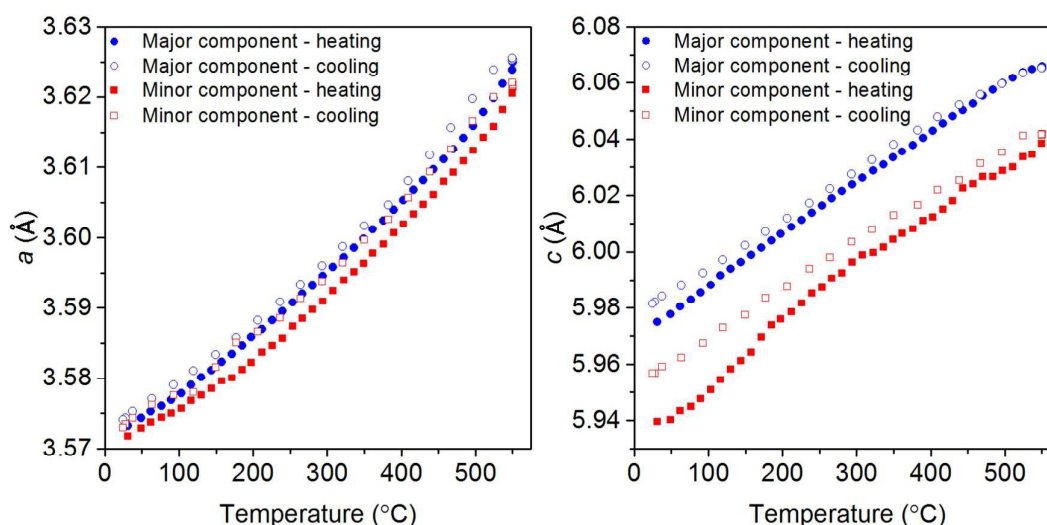

Figure 6 – Lattice parameters *a* and *c* for the two lithium-calcium imide components included in the refinement of the synchrotron diffraction data for the heating of lithium-calcium imide under flowing helium gas. Errors in the lattice parameter values are 1-2x10^{-4} Å.

Having established that, under an inert gas atmosphere, lithium-calcium imide is stable in the temperature range used for ammonia decomposition, a second experiment was conducted with the sample heated under ammonia flow. The experimental results are summarised in Figure 7, showing contour plots of sections of the diffraction data. These data indicate that, unlike under helium gas flow, the catalyst is not stable under ammonia flow. This is consistent with the *ex-situ* diffraction data which indicated that lithium amide and calcium imide were formed during the ammonia decomposition reaction.
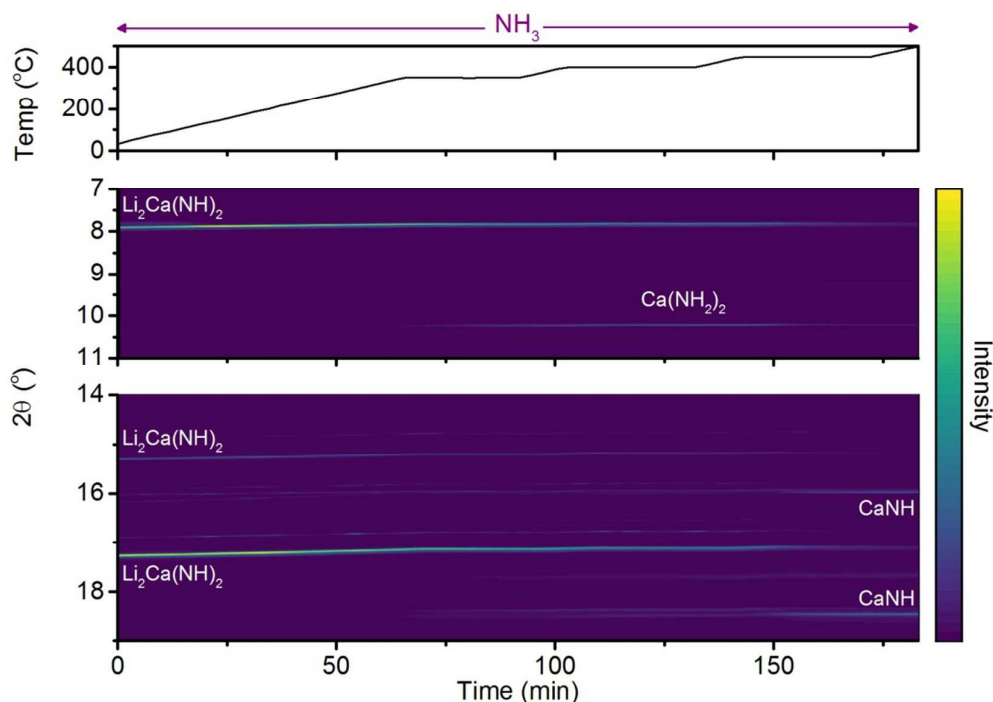
Figure 7 – Selected contour plots of synchrotron X-ray powder diffraction data for lithium-calcium imide heated under 1 sccm flowing ammonia gas.

The *in-situ* data show that the interaction of lithium-calcium imide with ammonia is more complex than a simple separation into lithium amide and calcium imide as may be surmised from the *ex-situ* analysis. The data from the experiment were analysed using the Rietveld method, and the resultant molar percentages extracted for each phase included in the refinement process are shown in Figure 8. The analysis of these data is complicated by overlapping Bragg peaks for lithium amide-imide, calcium imide and lithium-calcium imide, so a manual refinement of every fifth dataset was chosen instead of a batch refinement process as used in our previous *in-situ* studies[8].
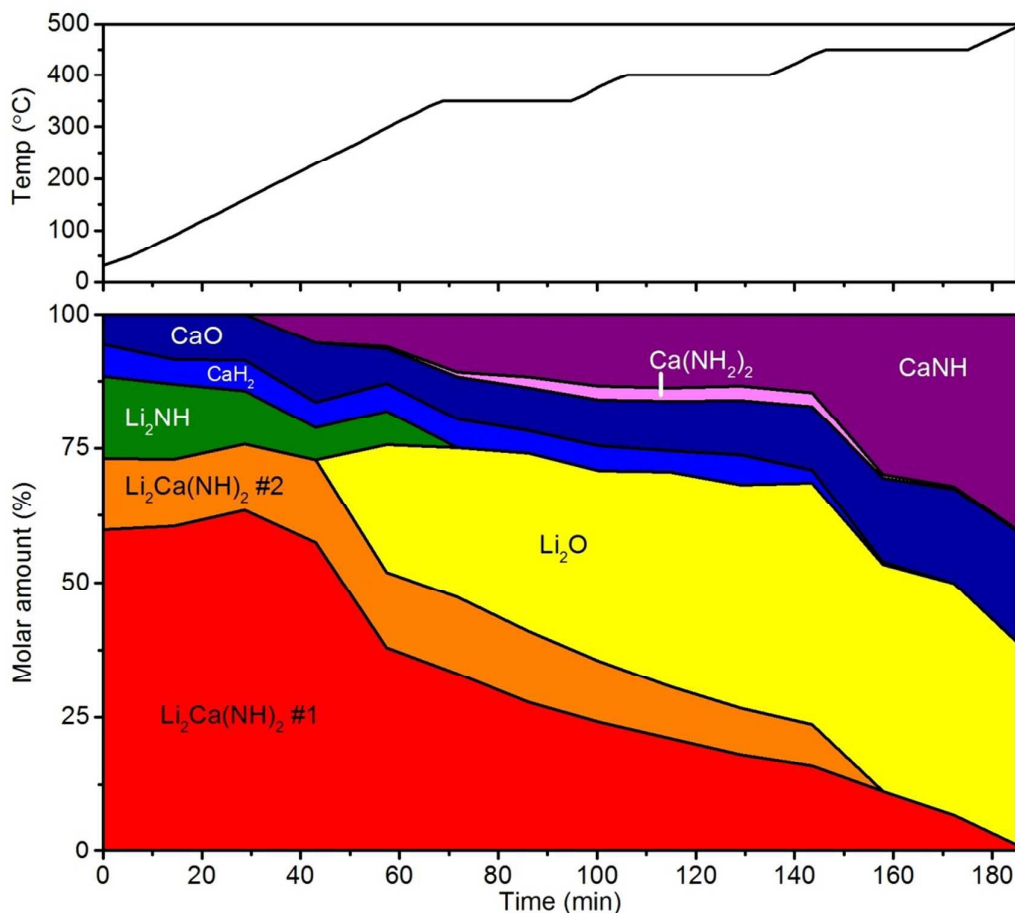
Figure 8 - Molar percentages of the crystalline phases present during exposure of lithium-calcium imide to ammonia, as extracted from Rietveld analysis of every fifth synchrotron X-ray powder diffraction data set. Li₂Ca(NH)₂ #1 is the major component of the lithium-calcium imide peak; Li₂Ca(NH)₂ #2 is the minor component.

Below 200 °C, the most significant change in the sample is the loss of the lithium imide impurity, which is most likely to have formed lithium amide by reaction with ammonia. Above 200 °C, the lithium-calcium imide begins to diminish, with calcium imide and lithium oxide phases growing in to replace it. Since lithium amide was not detected in the diffraction data at this stage, and the temperature is below its melting point, it was presumed that all of the lithium amide was oxidised by reaction with the sapphire capillary. Although sapphire has proven to be reasonably inert for the study of lithium amide systems, it clearly will react with lithium amide under certain conditions. Above 370 °C, no lithium amide formed from the decomposition of lithium-calcium imide will be observed, due to it being molten, and this should be taken into account when interpreting the data in Figure 8. However, it would appear that the lithium oxide phase may well be a good proxy for the amount of lithium amide formed from the decomposition of lithium-calcium imide; the molar ratio of lithium oxide to calcium imide at the end of the experiment is approximately 1:1, in keeping with the lithium-calcium ratio in the starting material. As the sample was cooled at the end of the experiment, a small amount of lithium amide was observed in the diffraction data, which is consistent with the proposed decomposition mechanism from lithium-calcium imide to calcium imide and lithium imide.

During the first dwell in temperature at 350 °C, a new Bragg peak is observed to form at 10.2°; this angular position is not indicative of the structures of lithium amide or calcium imide, the expected decomposition products. Rather, it matches the expected position of the (011) Bragg peak of calcium amide ($Ca(NH_2)_2$). The presence of calcium amide, even in the small quantity observed in this experiment, was unexpected, as the synthesis of calcium amide has typically required reactive ball-milling of calcium hydride under elevated ammonia pressure[24,25] or reaction between calcium metal and liquid ammonia over long timescales[26]. These data suggest that calcium amide can be formed from calcium imide under more moderate conditions than from calcium hydride or calcium metal.

Although the calcium imide molar amount in Figure 8 is presented as a single phase, close examination of the diffraction data toward the end of the experiment (i.e. at the highest temperatures studied) reveals complex lineshapes in the Bragg peaks associated with calcium imide, Figure 9a. In the Rietveld analysis of these data, these peak shapes were fitted using three calcium imide components. The presence of these complex lineshapes and their evolution in the context of the presence of ammonia may be indicative of stoichiometry variation associated with a non-stoichiometric calcium imide phase.
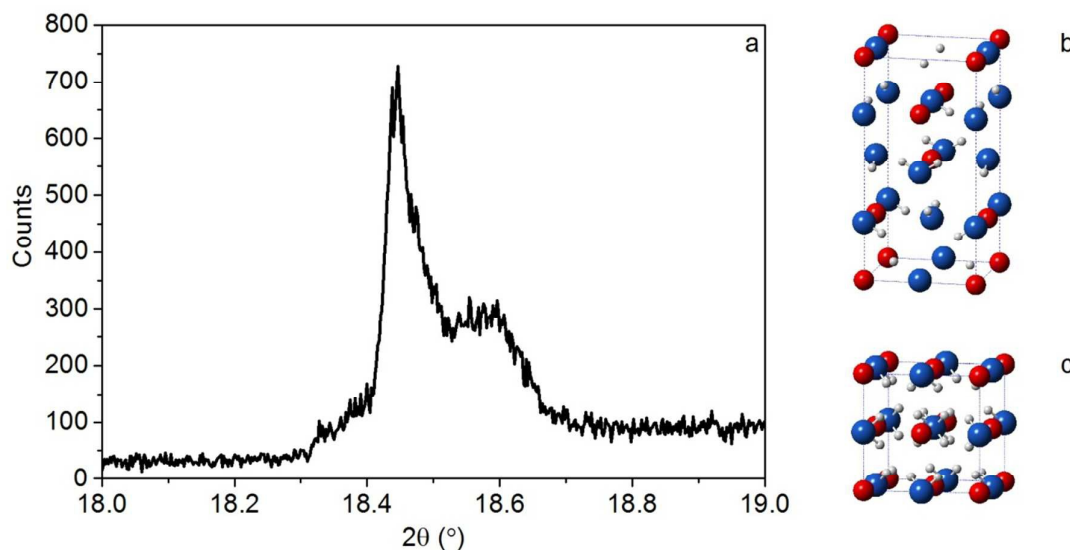

Figure 9 – a) Synchrotron X-ray diffraction data showing the (002) Bragg peak of calcium imide under flowing ammonia at 450 °C. Crystal structures of b) calcium amide and c) calcium imide showing calcium atoms in red, nitrogen in blue and hydrogen in grey.

Examining the crystal structures of calcium amide (as reported by Senker et al.[27]) and calcium imide, Figure 9b and c, it can be seen that calcium amide adopts a tetragonal structure where the amide groups form a pseudo-cubic close packed arrangement with the calcium ions occupying half of the octahedral holes in the structure. Calcium imide crystallises with imide ions in a close packed cubic array and calcium ions in all of the octahedral holes (the rock salt structure). Therefore, the calcium amide can be considered to be an ordered, half-occupied supercell of the calcium imide structure, in the same way that tetragonal lithium amide is an ordered supercell of the fluorite structure of lithium imide, where lithium ions occupy the tetrahedral, rather than the octahedral, sites in the close-packed cubic lattice. Given that this topological similarity facilitates the formation of non-stoichiometric phases by Frenkel defect migration in the lithium amide-imide system, it is reasonable to suggest that the same mechanism may be possible in the case of calcium amide-imide. Further

investigation would be required to confirm this hypothesis. The extensive oxidation of the sample observed above 450 °C precluded the investigation of the behaviour of the system at higher temperatures.

The behaviour of the lithium-calcium imide catalyst in the synchrotron diffraction experiment was mirrored in a combined DSC-TGA experiment, the results of which are plotted in Figure 10. The same endothermic event at 86 °C, as was observed under helium flow, was seen under ammonia, consistent with the lithium imide order-disorder transition. The sample began gaining mass at around 200 °C, consistent with the diffraction data and was correlated with a broad exothermic event in the data. The peak of this exothermic event coincides with a sharp endothermic event at 367 °C. This is consistent with the absorption of ammonia by lithium imide to form lithium amide (or lithium amide-like non-stoichiometric species), which melts at around 370 °C.
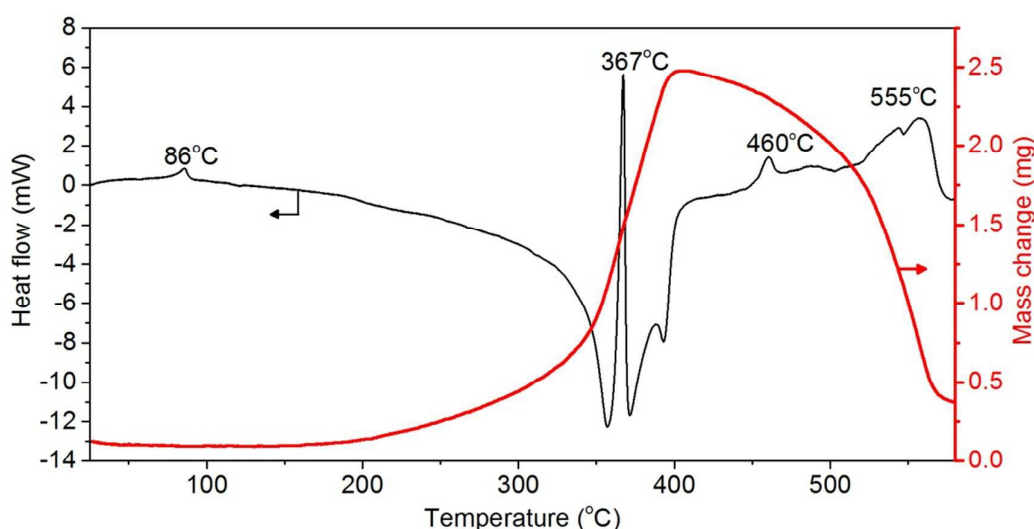

Figure 10 - Combined DSC-TGA experiment on lithium-calcium imide under 20 sccm flowing ammonia gas.

The maximum mass increase of 2.5 mg, reached at 400 °C, represents a 31 % gain over the starting sample mass of 8.7 mg. Considering the reaction of lithium imide to lithium amide, the release of the maximum amount of lithium imide from the structure (i.e. full decomposition to lithium imide and calcium imide) and its subsequent conversion to lithium amide would result in a mass increase of 20 %. Therefore, the larger mass increase observed in the DSC-TGA experiment is consistent with the additional formation of calcium amide and/or non-stoichiometric calcium imide, as observed in the diffraction experiment.

Above 400 °C, the mass decreases until the maximum temperature of the experiment, 575 °C. There are at least two endothermic events during the mass loss. Most of the mass loss occurs at temperatures which were not accessed in the synchrotron experiment and so cannot be related to those data. However, the mass appears to be returning to the initial mass value, which either suggests the formation of a mixture of lithium imide and calcium imide, the decomposed catalyst, or potentially the reformation of lithium-calcium imide.

The behaviour of the lithium-calcium imide catalyst under ammonia was investigated further in an *in-situ* neutron powder diffraction experiment. The use of neutrons allowed for a stainless steel

reactor to be used, removing the complication of the sample oxidising and thus allowing the higher temperature behaviour to be studied. A contour plot of the diffraction data from the 90 ° detector bank of the POLARIS instrument is shown in Figure 11, along with the sample temperature, gas composition and flow, and the ammonia conversion fraction, where applicable.

Initially, the sample of deuterated lithium-calcium imide was heated to 550 °C under flowing argon in order to examine whether exposing the sample to ammonia above the temperature where mass uptake was favourable would stabilise the lithium-calcium imide structure. It can be seen from the diffraction data that this is the case: when deuterated ammonia was added after five hours, the sample was essentially unchanged, remaining as lithium calcium imide. As such, the decomposition of the catalyst can be avoided in the same way as the conversion of lithium imide into lithium amide[8]. A relatively high ammonia conversion fraction of 0.6 was observed at this temperature, though the reactor geometry in the neutron diffraction experiment is not optimised to give the highest ammonia decomposition performance.
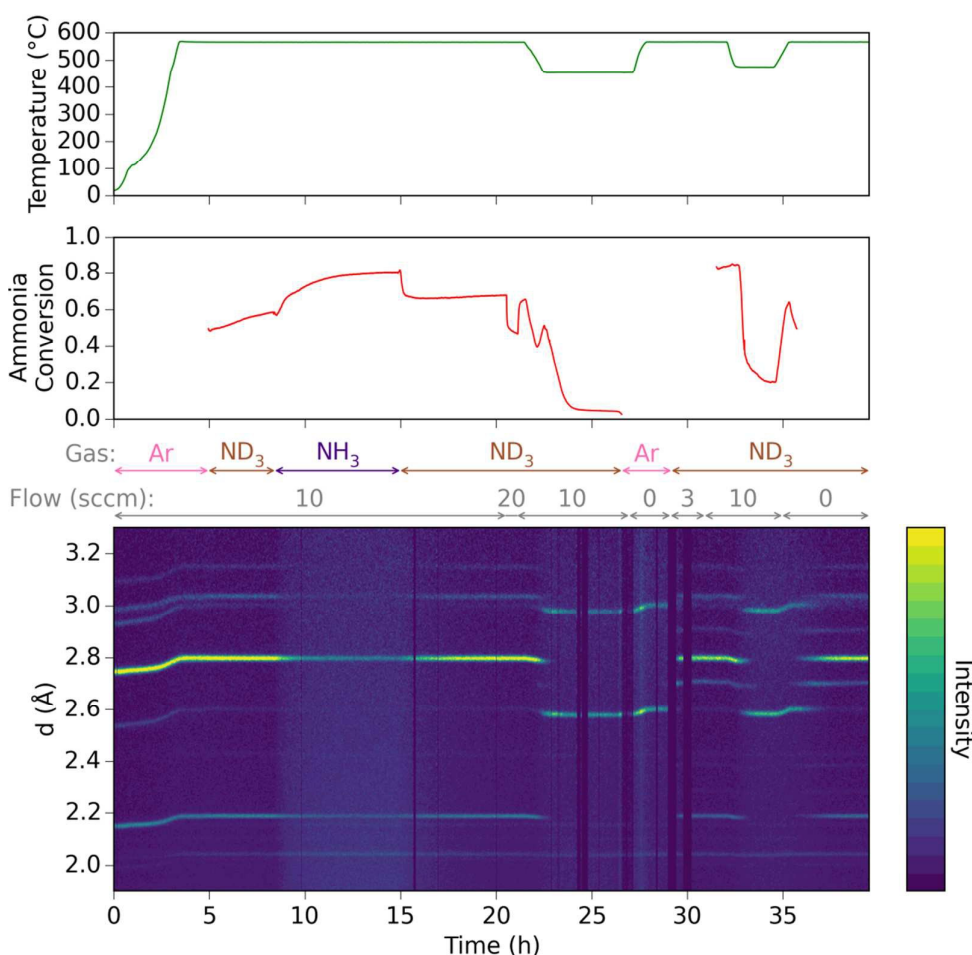

Figure 11 - Neutron powder diffraction experiment on deuterated lithium-calcium imide, showing (top) the sample temperature, (middle) the ammonia conversion fraction and (bottom) a contour plot of the diffraction data, with gas composition and flow indicated above. Gaps in the contour plot data represent periods where the ISIS synchrotron was not operational.

The lattice parameters of the lithium-calcium imide extracted from Rietveld analysis of the diffraction data during this period show that the exposure of the sample to ammonia resulted in a very slight (0.05 %) decrease in the *a* parameter and a larger increase (0.1 %) in the *c* parameter (see ESI). Based on our analysis of lithium imide-amide[8,22], these changes in the lattice parameters may indicate a degree of non-stoichiometry which can be accommodated in the lithium-calcium imide structure without causing the decomposition of the phase. More detailed analysis would be required to establish whether this was unambiguously the case.

Having observed that lithium-calcium imide can be stabilised under ammonia at high temperature, an isotope exchange experiment was then conducted. Approximately 8 hours into the experiment, the gas flow over the sample was switched from ND_3 to NH_3. At this point, and for the duration of the exchange, an increased background signal can be observed in the contour plot of the diffraction data along with a weaker signal from the sample, see Figure 11. This is consistent with the incorporation of hydrogen into the sample, as hydrogen has a very large incoherent neutron scattering cross section[28], which manifests as higher noise in diffraction data. In order to quantify the isotope exchange reaction, Rietveld analysis was performed which allowed the occupancy of the deuterium position in the lithium-calcium imide structure to vary completely between fully occupied by deuterium and fully occupied by hydrogen. The results of this analysis are shown in Figure 12.
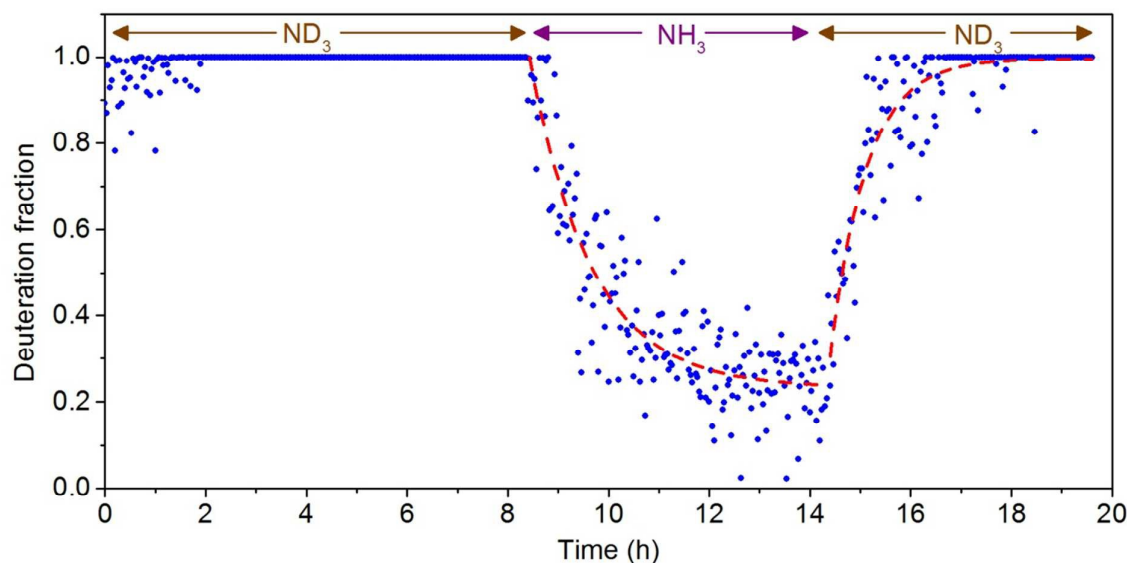

Figure 12 - Isotope exchange experiment during neutron powder diffraction of lithium-calcium imide, showing the deuteration fraction of the sample over time, with the gas species which the sample was exposed to indicated at the top of the figure. Red dashed lines are fits of the deuteration fraction data to simple exponential functions.

It can be seen that there is exchange of deuterium for hydrogen in the structure, with the deuteration fraction exhibiting an exponential decay, with a time constant of 74(2) minutes, after the NH_3 was introduced, down to a minimum of around 0.2. After approximately 14 hours experimental run time the flow was returned to ND_3, and the deuteration fraction returned to 1.0 with a more rapid time constant of 20(2) min. These data indicate that there is bulk interaction of the lithium-calcium imide sample with the ammonia flowing over and being decomposed by it. This bulk interaction shows how substantially the behaviour of amide- and imide-based ammonia decomposition catalysts differs from traditional surface catalysts.

Figure 13 presents the mass spectrometry data collected during the isotope exchange experiment. These data indicate that the ammonia decomposition rate is higher when the sample is not deuterated. This can be seen most clearly by examination of the nitrogen trace, which increases when the NH_3 is added, and decreases when the gas flow was switched back to ND_3. This variation gives some indication that there may be a kinetic isotope effect in this reaction, which would indicate that the rate determining step of the ammonia decomposition reaction using lithium-calcium imide involves a bond which contains H/D. A more detailed study of this effect, such as has been performed for sodium amide[11], would be needed to confirm that this is the case.
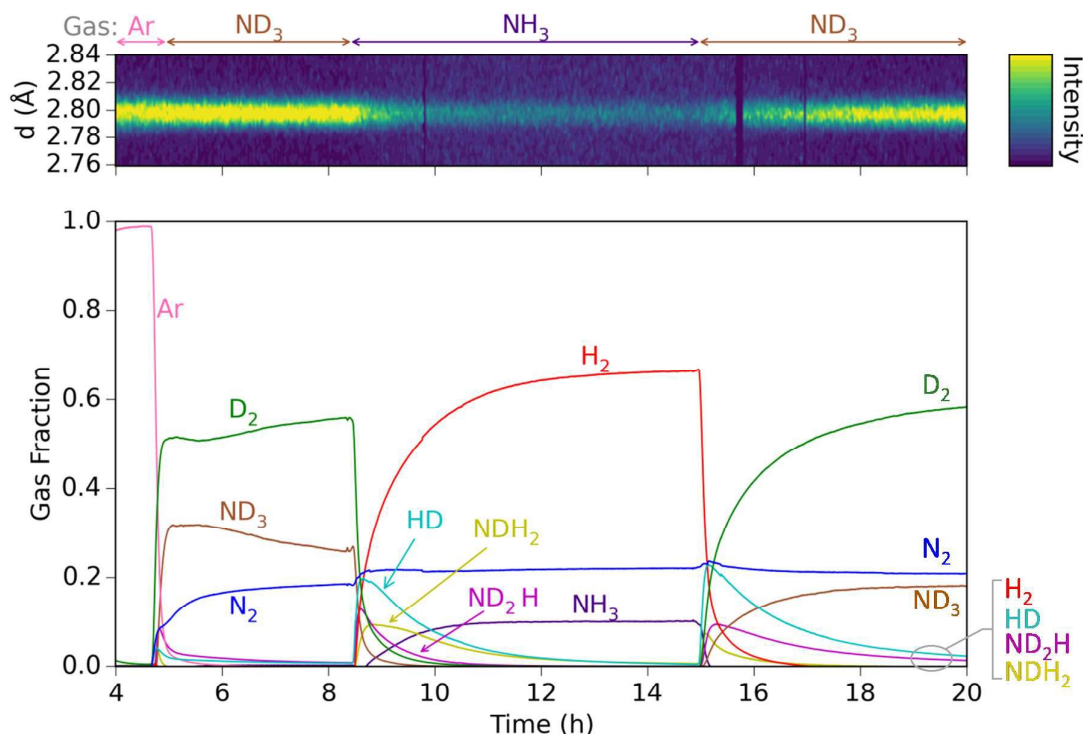

Figure 13 - Mass spectroscopy data during the isotope exchange reaction, with the neutron diffraction (011) Bragg peak of lithium-calcium imide shown for reference.

Following the isotope exchange reaction, the sample was cooled to 440 °C, whereupon the lithium-calcium imide phase disappeared and was replaced by calcium imide and, what is presumed to be, molten lithium amide. The absorption of ammonia associated with this transformation is observed in the apparent spike in the ammonia conversion fraction at approximately 23 hours. This result was consistent with the synchrotron and DSC-TGA data. At this point in the experiment, a blockage in the pipework formed which is most likely associated with the formation of molten lithium amide. By increasing the temperature of the sample to 550 °C and flowing argon across it, solid lithium imide was formed, which removed the blockage and allowed for the resumption of flowing ND_3. During this period, lithium-calcium imide was observed to reappear in the diffraction data. The reversibility of this transformation was confirmed by once again lowering and then raising the temperature of the sample, which resulted in the decomposition and reformation of the lithium-calcium imide catalyst before the system blocked again.

Conclusion

Lithium-calcium imide is a promising catalyst for the decomposition of ammonia for sustainable energy applications. It shows similar ammonia decomposition activity to lithium imide-amide and substantially improved containment of the catalyst mass within the reactor, making it the best-performing ammonia decomposition catalyst in this family studied to date.

The layered structure of lithium-calcium imide is susceptible to attack by ammonia to form lithium amide and calcium imide, as was observed by *in-situ* diffraction experiments. Evidence for the formation of non-stoichiometric calcium imide and calcium amide was observed in synchrotron X-ray diffraction and combined DSC-TGA experiments. At higher temperatures, after desorption of the absorbed ammonia, lithium-calcium imide was observed to reform. One way to consider this behaviour is that the ternary imide behaves in a very similar manner to the combination of its two imide components: the ammonia absorption behaviours of lithium and calcium imide are superimposed on the behaviour of the ternary imide. However the ternary structure does appear to raise the temperature at which the lithium imide layer reacts with ammonia compared with lithium imide alone.

While the presence of calcium imide and the reformation of lithium-calcium imide at high temperatures ensure that at least part of the catalyst remains solid over a wide range of ammonia decomposition reaction conditions, the formation of lithium amide is not ideal for the containment of the catalyst in a heated reactor. Furthermore, lithium amide will react with a number of common support materials, making the task of increasing the catalyst surface area more difficult. In the design of future metal amide and imide catalysts, one of the goals must be to find a catalyst which is solid and stable across the range of ammonia decomposition reaction conditions. It is possible that ternary imide structures, with two integrated metal ions, may provide a route to achieving this goal.

Financial Support

Acknowledgements

References

(1)   Reiter, A. J.; Kong, S.-C. *Energy Fuels* **2008**, *22*, 2963–2971.

(2)   Thomas, G.; Parks, G. *Potential Roles of Ammonia in a Hydrogen Economy*; U.S. Department of Energy: Washington, **2006**, 1-23.

(3)   Yin, S. F.; Xu, B. Q.; Zhou, X. P.; Au, C. T. *Appl. Catal., A* **2004**, *277*, 1–9.

(4)   Yin, S.; Xu, B.; Ng, C.; Au, C. *Appl. Catal., B* **2004**, *48*, 237–241.

Faraday Discussions Accepted Manuscript

(5)   Kowalczyk, Z.; Jodzis, S; Raróg, W.; Zieliński, J; Pielaszek, J., J. *Appl. Catal., A* **1998**, *173*, 153–160.

(6)   Raróg, W.; Kowalczyk, Z.; Sentek, J.; Składanowski, D.; Zieliński, J. *Catal. Lett.* **2000**, *68*, 163–168.

(7)   David, W. I. F.; Makepeace, J. W.; Callear, S. K.; Hunter, H. M. A.; Taylor, J. D.; Wood, T. J.; Jones, M. O. *J. Am. Chem. Soc.* **2014**, *136*, 13082–13085.

(8)   Makepeace, J. W.; Wood, T. J.; Hunter, H. M. A.; Jones, M. O.; David, W. I. F. *Chem. Sci.* **2015**, *6*, 3805–3815.

(9)   Guo, J.; Wang, P.; Wu, G.; Wu, A.; Hu, D.; Xiong, Z.; Wang, J.; Yu, P.; Chang, F.; Chen, Z.; Chen, P. *Angew. Chem. Int. Ed.* **2015**, *54*, 2950–2954.

(10)   Guo, J.; Chang, F.; Wang, P.; Hu, D.; Yu, P.; Wu, G.; Xiong, Z.; Chen, P. *ACS Catal.* **2015**, *5*, 2708–2713.

(11)   Wood, T. J.; Makepeace, J. W.; Hunter, H. M. A.; Jones, M. O.; David, W. I. F. *Phys. Chem. Chem. Phys.* **2015**, *17*, 22999–23006.

(12)   Gilbert, H. N.; Scott, N. D.; Zimmerli, W. F.; Hansley, V. L. *Ind. Eng. Chem.* **1933**, *25*, 735–741.

(13)   Chen, P.; Xiong, Z.; Luo, J.; Lin, J.; Tan, K. L. *Nature* **2002**, *420*, 302–304.

(14)   Leng, H.; Ichikawa, T.; Fujii, H. *J. Phys. Chem. B* **2006**, *110*, 12964–12968.

(15)   Nakamori, Y.; Kitahara, G.; Miwa, K.; Ohba, N.; Noritake, T.; Towata, S.; Orimo, S. *J. Alloys Compd.* **2005**, *404-406*, 396–398.

(16)   Tokoyoda, K.; Hino, S.; Ichikawa, T.; Okamoto, K.; Fujii, H. *J. Alloys Compd.* **2007**, *439*, 337–341.

(17)   Chu, H.; Xiong, Z.; Wu, G.; He, T.; Wu, C.; Chen, P. *Int. J. Hydrogen Energy* **2010**, *35*, 8317–8321.

(18)   Szmigiel, D.; Bielawa, H.; Kurtz, M.; Hinrichsen, O.; Muhler, M.; Raróg, W.; Jodzis, S.; Kowalczyk, Z.; Znak, L.; Zieliński, J. *J. Catal.* **2002**, *205*, 205–212.

(19)   Guo, J.; Chen, Z.; Wu, A.; Chang, F.; Wang, P.; Hu, D.; Wu, G.; Xiong, Z.; Yu, P.; Chen, P. *Chem. Commun.* **2015**, *51*, 15161–15164.

(20)   Balogh, M. P.; Jones, C. Y.; Herbst, J. F.; Hector, L. G.; Kundrat, M. *J. Alloys Compd.* **2006**, *420*, 326–336.

(21)   David, W. I. F.; Jones, M. O.; Gregory, D. H.; Jewell, C. M.; Johnson, S. R.; Walton, A.; Edwards, P. P. *J. Am. Chem. Soc.* **2007**, *129*, 1594–1601.

(22)   Makepeace, J. W.; Jones, M. O.; Callear, S. K.; Edwards, P. P.; David, W. I. F. *Phys. Chem. Chem. Phys.* **2014**, *16*, 4061-4070.

(23)   Bull, D. J.; Weidner, E.; Shabalin, I. L.; Telling, M. T. F.; Jewell, C. M.; Gregory, D. H.; Ross, D. K. *Phys. Chem. Chem. Phys.* **2010**, *12*, 2089–2097.

(24)   Hino, S.; Ichikawa, T.; Leng, H.; Fujii, H. *J. Alloys Compd.* **2005**, *398*, 62–66.

(25)   Leng, H. Y.; Ichikawa, T.; Hino, S.; Hanada, N.; Isobe, S.; Fujii, H. *J. Power Sources* **2006**, *156*, 166–170.

(26)   Senker, J.; Jacobs, H.; Müller, M.; Press, W.; Mayer, H. M.; Ibberson, R. M. *Z. Anorg. Allg. Chem.* **1999**, *625*, 2025–2032.

(27)   Senker, J.; Jacobs, H.; Müller, M.; Press, W.; Mayer, H. M.; Ibberson, R. M. *J. Phys. Chem. B* **1998**, *102*, 931–940.

(28)   National Institute of Standards and Technology. *Neutron scattering lengths and cross sections* http://www.ncnr.nist.gov/resources/n-lengths/ (accessed Nov 16, 2015).